



Differential expression and prognostic relevance of autophagy-related markers ATG4B, GABARAP, and LC3B in breast cancer

Svetlana Bortnik¹ · Basile Tessier-Cloutier² · Samuel Leung² · Jing Xu^{1,3} · Karama Asleh² · Samantha Burugu² · Jamie Magrill² · Kendall Greening² · Fatemeh Derakhshan² · Stephen Yip² · Tony Ng² · Karen A. Gelmon^{4,5} · Torsten O. Nielsen² · Sharon M. Gorski^{1,3}

Received: 20 December 2019 / Accepted: 8 July 2020 / Published online: 20 July 2020
© Springer Science+Business Media, LLC, part of Springer Nature 2020

Abstract

Purpose Previous studies indicate that breast cancer molecular subtypes differ with respect to their dependency on autophagy, but our knowledge of the differential expression and prognostic significance of autophagy-related biomarkers in breast cancer is limited.

Methods Immunohistochemistry (IHC) was performed on tissue microarrays from a large population of 3992 breast cancer patients divided into training and validation cohorts. Consensus staining scores were used to evaluate the expression levels of autophagy proteins LC3B, ATG4B, and GABARAP and determine the associations with clinicopathological variables and molecular biomarkers. Survival analyses were performed using the Kaplan–Meier function and Cox proportional hazards regression models.

Results We found subtype-specific expression differences for ATG4B, with its expression lowest in basal-like breast cancer and highest in Luminal A, but there were no significant associations with patient prognosis. LC3B and GABARAP levels were highest in basal-like breast cancers, and high levels were associated with worse outcomes across all subtypes (DSS; GABARAP: HR 1.43, LC3B puncta: HR 1.43). High ATG4B levels were associated with ER, PR, and BCL2 positivity, while high LC3B and GABARAP levels were associated with ER, PR, and BCL2 negativity, as well as EGFR, HER2, HER3, CA-IX, PD-L1 positivity, and high Ki67 index ($p < 0.05$ for all associations). Exploratory multi-marker analysis indicated that the combination of ATG4B and GABARAP with LC3B could be useful for further stratifying patient outcomes.

Conclusions ATG4B levels varied across breast cancer subtypes but did not show prognostic significance. High LC3B expression and high GABARAP expression were both associated with poor prognosis and with clinicopathological characteristics of aggressive disease phenotypes in all breast cancer subtypes.

Keywords ATG4B · Autophagy · Biomarker · Breast cancer · GABARAP · Immunohistochemistry · LC3B · Prognosis · Subtype

Electronic supplementary material The online version of this article (<https://doi.org/10.1007/s10549-020-05795-z>) contains supplementary material, which is available to authorized users.

✉ Sharon M. Gorski
sgorski@bcgsc.ca

¹ Canada's Michael Smith Genome Sciences Centre, BC Cancer, Vancouver, BC, Canada

² Department of Pathology and Laboratory Medicine, University of British Columbia, Vancouver, BC, Canada

³ Department of Molecular Biology and Biochemistry, Simon Fraser University, Burnaby, BC, Canada

⁴ Medical Oncology, BC Cancer, Vancouver, BC, Canada

⁵ Department of Medicine, UBC, Vancouver, BC, Canada

Abbreviations

AIC	Akaike information criterion
ATG	Autophagy-related
ATG4B	Autophagy-related 4B
BCL2	B-cell lymphoma 2
CA-IX	Carbonic anhydrase 9
DSS	Disease-specific survival
EGFR	Epidermal growth factor receptor
ER	Estrogen receptor
FDA	Food and Drug Administration
GABARAP	GABA type A receptor-associated protein
GATE-16	Golgi-associated ATPase enhancer of 16 kDa

GABARAPL2	GABA type A receptor-associated protein like 2
HER2	Human epidermal growth factor receptor 2
HER3	Human epidermal growth factor receptor 3
HR	Hazard ratio
IHC	Immunohistochemistry
LC3B	Microtubule associated protein 1 light chain 3 beta
OS	Overall survival
PD-L1	Programmed death-ligand 1
PE	Phosphatidylethanolamine
PR	Progesterone receptor
RFS	Relapse-free survival
TMA	Tissue microarray
TNBC	Triple-negative breast cancer
TNP	Triple-negative phenotype

Introduction

Macroautophagy (herein autophagy) is an evolutionarily conserved lysosome-mediated degradation and recycling process shown to contribute to both tumor suppression and tumor progression, depending primarily on the stage of tumorigenesis [1–3]. In advanced malignancies, autophagy promotes cancer cell survival and contributes to cancer progression and drug resistance, hence becoming a promising target for anticancer therapy [1–3]. Recent preclinical and clinical trial findings have led to a resurgent interest in anticancer autophagy inhibition strategies [4], driving an accompanying need to better understand the potential biomarker utility of autophagy proteins. Autophagy is a multi-step process that involves more than 30 core autophagy-related (ATG) proteins [5–7]. These proteins act to initiate, elongate, and complete the formation of double-membrane structures called autophagosomes that encapsulate portions of cytoplasm. Autophagosomes fuse with lysosomes to form autolysosomes where the contents are degraded, released and recycled by the cell [1, 8, 9].

Among the key autophagy proteins are the Atg8 and ATG4 families. In mammals, the Atg8 family of ubiquitin-like proteins is represented by two subfamilies: the microtubule-associated protein 1 light chain 3 (MAP1LC3, or LC3) subfamily, consisting of LC3A, LC3B, LC3B2, and LC3C, and the gamma-aminobutyric acid receptor-associated protein (GABARAP) subfamily that includes GABARAP, GABARAPL1, and Golgi-associated ATPase enhancer of 16 kDa (GATE-16)/GABARAPL2 [10]. Each family member, while demonstrating some functional redundancy with other members, plays distinct roles in the autophagy process [11, 12]. For example, LC3s are required for the elongation

step [11, 13], whereas GABARAPs were shown to play important roles in autophagy initiation [13] and autophagosome closure [11]. The LC3 and GABARAP proteins are processed by the ATG4B cysteine protease at two different steps in the autophagy process. First, ATG4B cleaves the carboxyl terminus of newly synthesized pro-LC3 to generate LC3-I [14] enabling its conjugation to phosphatidylethanolamine (PE) to form membrane-bound LC3-II, which is required for autophagosome elongation. Second, ATG4B functions in delipidation of LC3-II from the autophagosome membrane to ensure recycling of LC3-I in the cell [15]. Other ATG4 family members (ATG4A, ATG4C, and ATG4D) have been described in mammalian cells, though ATG4B displays the broadest substrate specificity and greatest affinity for pro-LC3B [16–18] and can also process other family members including GABARAP. ATG4B has become an attractive therapeutic target [19–25], and several preclinical studies reported ATG4B inhibition as an effective strategy to sensitize cancer cells to chemotherapy [19, 26–28].

A variety of strategies to develop clinical biomarkers for monitoring autophagy in cancer patients are under investigation. Due to the dynamic nature of autophagy, complexity of its regulation, and autophagy-independent roles of ATG proteins, the assessment of several different markers in the same patient has been recommended. The most common biomarker approach explored to date in various cancers is the immunohistochemical analysis of autophagy proteins, particularly LC3B, in tumor tissue (reviewed in [3, 29]). While the overall levels of LC3B were investigated previously in many different tumor types, only a few more recent studies [30–33] distinguished between the processed forms of LC3B, namely cytosolic (LC3B-I) and membrane-bound (LC3B-II, or LC3B “puncta”) forms. Only an LC3B punctate pattern in cells represents the membrane-bound LC3B-PE form and can be used to infer levels of autophagosomes [34, 35].

By RNA expression profile, breast cancer is classified into four main molecular subtypes, namely Luminal A (Lum A), Luminal B (Lum B), basal-like, and HER2-enriched. Alternative clinical and immunohistochemical sub-classifications have been described, including triple-negative breast cancer (TNBC), which is immunohistochemically negative for ER, PR, and HER2 receptors. Although often used interchangeably with basal-like, it is only approximately 70–75% of TNBC that has a basal-like expression profile [36, 37]. These distinct breast cancer subtypes have shown differential sensitivity to autophagy modulation [26, 38, 39], but our knowledge of autophagy protein expression and biomarker potential in breast cancer is still limited.

Here, we report the differential expression levels of ATG4B, GABARAP, and LC3B in the major breast cancer subtypes. We demonstrate significant associations between these autophagy-related proteins, clinicopathological

characteristics of the disease, and established biomarkers. In addition, following the reporting recommendations for tumor marker prognostic studies (REMARK) [40], we report the prognostic values of ATG4B, GABARAP, and LC3B alone and in combination in a large cohort of breast cancer patients.

Results

Patient demographics and pathologic data

In our cohort of 3992 breast cancer patients, split into training and validation sets (see Sect. 2), the mean age at diagnosis was 59.1 years, and the median follow-up time (the time of diagnosis to time of event or last follow-up) was 12.6 years; the range for follow-up was 1 month to 18.5 years (Supplementary Table S1). The median tumor size was 2 cm; 53.5% of patients had grade 3 tumors, 43% were node positive, 70% were ER positive, and 13% were HER2 positive. Adjuvant systemic therapy was given to 58% (Supplementary Table S1). Tables 1, 2, 3 and Supplementary Table S2 show summary statistics of clinicopathological variables of interest split by ATG4B, GABARAP, and LC3B status. The values highlighted below are those from the validation cohort and include only those results that were independently significant in both training and validation sets unless otherwise stated (see Sect. 2). The separate results for training and combined cohorts are provided in Supplementary Tables S3, S4, and S6.

Differential ATG4B expression across breast cancer subtypes and biomarker associations

To determine the clinical relevance of ATG4B expression in breast cancer, we examined ATG4B cytoplasmic staining (Fig. 1) in our cohort and evaluated its association with breast cancer biomarkers. As shown in Figs. 2 and 3, ATG4B was detected at significantly lower levels in ER–/PR–/HER2– (triple-negative, TNP) vs. non-triple-negative breast cancers ($p < 0.0001$), and basal-like vs. non-basal molecular subtypes ($p = 0.003$). ATG4B expression did not significantly correlate with patient age at diagnosis, tumor size, or nodal status. However, as shown in Table 1, Fig. 3, and Supplementary Table S3, there was a significant association between ATG4B protein expression and lower tumor grade ($p < 0.0001$) and ER and PR positivity ($p < 0.0001$). In addition, there was a significant positive association between ATG4B and BCL2 ($p = 0.02$). There was a negative association between ATG4B and EGFR ($p = 0.02$), as well as ATG4B and Ki67 ($p = 0.008$).

In our patient cohort, the common clinicopathologic variables including patient age at diagnosis, tumor size,

histologic grade, nodal status, ER/PR/HER2 status, and Ki67 expression were all statistically significant predictors of overall survival (OS), disease-specific survival (DSS), and relapse-free survival (RFS) on univariate survival analysis (Supplementary Table S5). ATG4B expression was not found to be significantly associated with patient prognosis (Supplementary Table S4).

Differential GABARAP expression across breast cancer subtypes, biomarker associations, and association with poor prognosis

To determine the clinical relevance of GABARAP expression in breast cancer, we scored its cytoplasmic staining pattern (Fig. 1, Supplementary Fig. S1) and evaluated its association with known biomarkers and patient survival. As shown in Fig. 2, basal-like and triple-negative breast cancers had the highest expression levels of GABARAP across all breast cancer subtypes. High GABARAP expression was associated with markers of a more aggressive phenotype, such as larger tumor size, negative ER and PR status, positive EGFR and CK5/6 expression, HER2 and HER3 positivity, high Ki67, low BCL2, high IGF1R expression, as well as high PD-L1 and CA-IX expression (Table 2, Fig. 4, Supplementary Table S3). All of these marker associations were statistically significant ($p < 0.05$ for all associations) in the validation cohort. High GABARAP expression levels were associated with poor overall survival and disease-specific survival in the validation cohort at 5- and 10-years cutpoints of follow-up time (Fig. 5a, Table 4): HR 1.27 (95% CI 1.06–1.52), $p = 0.009$ for OS at 10 years; HR 1.48 (95% CI 1.15–1.92), $p = 0.002$ for OS at 5 years; HR 1.43 (95% CI 1.15–1.80), $p = 0.001$ for DSS at 10 years; HR 1.69 (95% CI 1.25–2.32), $p < 0.001$ for DSS at 5 years. There were no breast cancer subtype-specific survival associations with GABARAP that were statistically significant in both training and validation cohorts (Supplementary Table S4). To determine if GABARAP expression was an independent marker of prognosis, we performed multivariable analyses with all clinicopathological parameters. GABARAP expression was not found to be an independent prognostic factor ($p > 0.05$) (Table 5, Supplementary Table S6).

High diffuse or punctate LC3B expression is associated with predictors of more aggressive phenotype and poor prognosis in breast cancer

To evaluate LC3B biomarker potential in this large cohort, we scored both diffuse (H-score) and punctate staining patterns (Fig. 1). Among all intrinsic subtypes, basal-like breast cancers had the highest levels of both punctate and diffuse LC3B (Fig. 2). Higher LC3B expression (H-score and puncta score) was significantly associated with several

Table 1 Univariable associations of ATG4B (H-score > 150) with other markers and predictors of prognosis (validation cohort)

Variable	Levels <i>N</i>	≤ 150 1093	> 150 324	Total 1989	<i>p</i> value OneWay_Test
Age at diagnosis	Mean (SE)	58 (0)	58 (1)	59 (0)	0.589
	Median (IQR)	59 (48–69)	58 (47–68)	59 (48–69)	
	Missing	0	0	0	
Tumor size (cm)	Mean (SE)	3 (0)	2 (0)	2 (0)	0.0495
	Median (IQR)	2 (2–3)	2 (2–3)	2 (2–3)	
	Missing	6	3	16	
PearsonChi_square					
Tumor grade	Grade 1–2	420 (40%)	157 (51%)	577 (42%)	8e–04
	Grade 3	633 (60%)	152 (49%)	785 (58%)	
	Missing	40	15	85	
Nodal status	Negative	612 (56%)	182 (56%)	794 (56%)	1.000
	Positive	478 (44%)	142 (44%)	620 (44%)	
	Missing	3	0	5	
ER	< 1%	343 (31%)	64 (20%)	407 (29%)	6e–05
	≥ 1%	747 (69%)	260 (80%)	1007 (71%)	
	Missing	3	0	14	
PR	< 1%	556 (53%)	110 (35%)	666 (49%)	0.000
	≥ 1%	484 (47%)	202 (65%)	686 (51%)	
	Missing	53	12	216	
HER2	{0, 1 +, 2 + w/FISH – ve}	919 (86%)	273 (86%)	1192 (86%)	1.000
	{2 + w/FISH + ve, 3 +}	151 (14%)	45 (14%)	196 (14%)	
	Missing	23	6	97	
CK5/6	Negative	874 (90%)	264 (92%)	1138 (90%)	0.469
	Positive	97 (10%)	24 (8%)	121 (10%)	
	Missing	122	36	306	
EGFR	Negative	829 (85%)	267 (91%)	1096 (86%)	0.016
	Positive	149 (15%)	28 (9%)	177 (14%)	
	Missing	115	29	274	
Ki67	< 14%	512 (52%)	183 (60%)	695 (54%)	0.008
	≥ 14%	482 (48%)	120 (40%)	602 (46%)	
	Missing	99	21	266	
BCL2	Negative or ≤ 10%	297 (28%)	67 (21%)	364 (26%)	0.017
	Any staining and > 10%	771 (72%)	253 (79%)	1024 (74%)	
	Missing	25	4	164	
CA-IX	Negative	849 (83%)	263 (85%)	1112 (83%)	0.594
	Any positive	173 (17%)	48 (15%)	221 (17%)	
	Missing	71	13	181	
HER3 (any staining)	No staining	774 (88%)	244 (92%)	1018 (89%)	0.119
	Any staining	105 (12%)	22 (8%)	127 (11%)	
	Missing	214	58	431	
IGF1R (Allred ≥ 7)	< 7	584 (57%)	173 (56%)	757 (57%)	0.844
	≥ 7	437 (43%)	134 (44%)	571 (43%)	
	Missing	72	17	337	
PD-L1 (≥ 1%)	< 1	909 (92%)	285 (92%)	1194 (92%)	1.000
	≥ 1	81 (8%)	26 (8%)	107 (8%)	
	Missing	103	13	534	

Table 1 (continued)

					PearsonChi_square
Basal	Non-basal	896 (88%)	284 (94%)	1180 (90%)	0.003
	Basal	119 (12%)	17 (6%)	136 (10%)	
	Missing	78	23	273	
Triple-negative	Not TNP	874 (81%)	294 (92%)	1168 (84%)	1e-05
	TNP	202 (19%)	26 (8%)	228 (16%)	
	Missing	17	4	84	
IHC subtype	lumA	418 (41%)	158 (52%)	576 (44%)	0.000
	lumB/ki67 high	248 (24%)	73 (24%)	321 (24%)	
	lumB/HER2+	63 (6%)	20 (7%)	83 (6%)	
	HER2+ /ER- /PR-	84 (8%)	24 (8%)	108 (8%)	
	Basal	119 (12%)	17 (6%)	136 (10%)	
	add'l TNP	83 (8%)	9 (3%)	92 (7%)	
	Missing	78	23	273	
GABARAP (H-score > 175)	≤ 175	361 (34%)	94 (30%)	455 (33%)	0.167
	> 175	697 (66%)	222 (70%)	919 (67%)	
	Missing	35	8	423	
LC3B (H-score > 150)	≤ 150	356 (35%)	85 (28%)	441 (33%)	0.024
	> 150	667 (65%)	222 (72%)	889 (67%)	
	Missing	70	17	528	
LC3B (puncta low/neg)	{D,E}	384 (38%)	113 (37%)	497 (37%)	0.870
	{A,B,C}	639 (62%)	194 (63%)	833 (63%)	
	Missing	70	17	528	
Adjuvant systemic therapy	No AST	458 (42%)	143 (44%)	601 (42%)	0.775
	TAM only	329 (30%)	100 (31%)	429 (30%)	
	Chemo only	219 (20%)	63 (19%)	282 (20%)	
	TAM + chemo	80 (7%)	16 (5%)	96 (7%)	
	Ovarian ablation or horm other than TAM; no chemo	3 (0%)	1 (0%)	4 (0%)	
	Ovarian ablation or horm other than TAM + chemo	4 (0%)	1 (0%)	5 (0%)	

clinicopathological variables characteristic of a more aggressive phenotype (Table 3, Fig. 6, Supplementary Table S3), including higher tumor grade, lymphovascular invasion, ER/PR negativity, positive HER2, HER3, CK5/6, EGFR, and CA-IX expression, as well as high Ki67 index. There was a statistically significant positive association between LC3B and GABARAP ($p \leq 0.0001$); no statistically significant association between LC3B and ATG4B, or between GABARAP and ATG4B was established. As shown in Fig. 5b–d and Table 4, high diffuse expression of LC3B was associated with poor DSS at 18 years (HR 1.31 (95% CI 1.07–1.61), $p=0.009$) and poor OS, DSS and RFS at 10 years and 5 years ($p < 0.05$ and $p \leq 0.003$; Table 4); high puncta levels of LC3B were associated with poor RFS at 5 years (HR 1.41 (95% CI 1.13–1.76), $p=0.002$) and with poor OS and DSS at 5-, 10- and 18-year

cutpoints of follow-up time (Fig. 5a, Table 4): HR 1.22 (95% CI 1.02–1.46), $p=0.027$ for OS at 10 years; HR 1.56 (95% CI 1.21–2.03), $p < 0.001$ for OS at 5 years; HR 1.43 (95% CI 1.14–1.79), $p=0.001$ for DSS at 10 years; HR 1.99 (95% CI 1.46–2.75), $p < 0.001$ for DSS at 5 years. There were no subtype-specific survival associations with LC3B that were statistically significant in both training and validation cohorts (Supplementary Table S4). To determine if LC3B was an independent prognostic marker, we performed multivariable analyses with all clinicopathological parameters. We found that LC3B puncta, but not LC3B H-score, was significantly associated with OS and DSS outcomes in the training cohort ($p < 0.001$ at 18-, 10- and 5-years) and combined cohort ($p < 0.006$ at 18, 10, and 5 years), but did not independently validate ($p > 0.05$) (Table 5, Supplementary Table S6).

Table 2 Univariable associations of GABARAP (H-score > 175) with other markers and predictors of prognosis (validation cohort)

Variable	Levels	≤ 175	> 175	Total	<i>p</i> value
	<i>N</i>	538	1028	1989	OneWay_Test
Age at diagnosis	Mean (SE)	59 (1)	58 (0)	59 (0)	0.148
	Median (IQR)	60 (49–69)	59 (47–69)	59 (48–69)	
	Missing	0	0	0	
Tumor size (cm)	Mean (SE)	2 (0)	3 (0)	2 (0)	0.038
	Median (IQR)	2 (2–3)	2 (2–3)	2 (2–3)	
	Missing	1	10	16	
PearsonChi_square					
Tumor grade	Grade 1–2	263 (51%)	391 (40%)	654 (43%)	4e–05
	Grade 3	255 (49%)	597 (60%)	852 (57%)	
	Missing	20	40	85	
Nodal status	Negative	312 (58%)	565 (55%)	877 (56%)	0.311
	Positive	226 (42%)	459 (45%)	685 (44%)	
	Missing	0	4	5	
ER	< 1%	90 (17%)	367 (36%)	457 (29%)	0.000
	≥ 1%	448 (83%)	657 (64%)	1105 (71%)	
	Missing	0	4	14	
PR	< 1%	192 (38%)	533 (55%)	725 (49%)	0.000
	≥ 1%	313 (62%)	434 (45%)	747 (51%)	
	Missing	33	61	216	
HER2	{0, 1+, 2+ w/FISH –ve}	480 (91%)	838 (84%)	1318 (86%)	8e-05
	{2+ w/FISH +ve, 3+}	46 (9%)	162 (16%)	208 (14%)	
	Missing	12	28	97	
CK5/6	Negative	449 (95%)	799 (89%)	1248 (91%)	0.000
	Positive	24 (5%)	101 (11%)	125 (9%)	
	Missing	65	128	306	
EGFR	Negative	452 (94%)	742 (82%)	1194 (86%)	0.000
	Positive	28 (6%)	166 (18%)	194 (14%)	
	Missing	58	120	274	
Ki67	< 14%	348 (72%)	421 (45%)	769 (54%)	0.000
	≥ 14%	137 (28%)	507 (55%)	644 (46%)	
	Missing	53	100	266	
BCL2	Negative or ≤ 10%	96 (18%)	312 (31%)	408 (27%)	0.000
	Any staining and > 10%	435 (82%)	687 (69%)	1122 (73%)	
	Missing	7	29	164	
CA-IX	Negative	436 (88%)	794 (82%)	1230 (84%)	0.007
	Any positive	61 (12%)	173 (18%)	234 (16%)	
	Missing	41	61	181	
HER3 (any staining)	No staining	417 (93%)	699 (87%)	1116 (89%)	0.001
	Any staining	30 (7%)	106 (13%)	136 (11%)	
	Missing	91	223	431	
IGF1R (Allred ≥ 7)	< 7	296 (60%)	504 (54%)	800 (56%)	0.046
	≥ 7	197 (40%)	423 (46%)	620 (44%)	
	Missing	45	101	337	
PD-L1 (≥ 1%)	< 1	460 (97%)	812 (89%)	1272 (92%)	0.000
	≥ 1	12 (3%)	96 (11%)	108 (8%)	
	Missing	66	120	534	

Table 2 (continued)

					PearsonChi_square
Basal	Non-basal	468 (96%)	818 (86%)	1286 (90%)	0.000
	Basal	17 (4%)	130 (14%)	147 (10%)	
	Missing	53	80	273	
Triple-negative	Not TNP	490 (92%)	789 (78%)	1279 (83%)	0.000
	TNP	41 (8%)	217 (22%)	258 (17%)	
	Missing	7	22	84	
IHC subtype	lumA	303 (62%)	328 (35%)	631 (44%)	0.000
	lumB/ki67 high	97 (20%)	247 (26%)	344 (24%)	
	lumB/HER2+	22 (5%)	64 (7%)	86 (6%)	
	HER2+ /ER- /PR-	22 (5%)	92 (10%)	114 (8%)	
	Basal	17 (4%)	130 (14%)	147 (10%)	
	add'l TNP	24 (5%)	87 (9%)	111 (8%)	
	Missing	53	80	273	
ATG4B (H-score > 150)	≤ 150	361 (79%)	697 (76%)	1058 (77%)	0.167
	> 150	94 (21%)	222 (24%)	316 (23%)	
	Missing	83	109	572	
LC3B (H-score > 150)	≤ 150	288 (60%)	193 (21%)	481 (34%)	0.000
	> 150	193 (40%)	747 (79%)	940 (66%)	
	Missing	57	88	528	
LC3B (puncta low/ neg)	{D,E}	259 (54%)	274 (29%)	533 (38%)	0.000
	{A,B,C}	222 (46%)	666 (71%)	888 (62%)	
	Missing	57	88	528	
Adjuvant systemic therapy	No AST	227 (42%)	431 (42%)	658 (42%)	0.104
	TAM only	185 (34%)	301 (29%)	486 (31%)	
	Chemo only	90 (17%)	220 (21%)	310 (20%)	
	TAM + chemo	35 (7%)	69 (7%)	104 (7%)	
	Ovarian ablation or horm other than TAM; no chemo	1 (0%)	3 (0%)	4 (0%)	
	Ovarian ablation or horm other than TAM + chemo	0 (0%)	4 (0%)	4 (0%)	

Multi-marker expression exploratory analysis: patients with high LC3B puncta, high GABARAP, and low ATG4B expression have the poorest prognosis

To determine if the combination of ATG4B, LC3B, and GABARAP can provide additional information regarding patient survival, we performed exploratory multi-marker analyses in the whole cohort. After combining all three markers (Fig. 5e), patients with high LC3B puncta expression (A,B,C puncta expression; denoted L+) tumors had an inferior prognosis compared to those with low LC3B puncta expression (D,E puncta expression; denoted L-) tumors, which prompted us to further analyze the patients within the L+ and L- subgroups according to GABARAP

and ATG4B expression. Within the L+ subgroup, high GABARAP expression (GABARAP H-score > 175; denoted G+) patients had significantly worse prognosis than low GABARAP expression (GABARAP H-score ≤ 175; denoted G-) patients (HR for 10-year DSS was 1.3 (1.05–1.61), $p = 0.0144$; HR for 10-year PFS was 1.48 (1.13–1.96), $p = 0.0034$), while patients with high ATG4B expression (ATG4B H-score > 150 denoted A+) demonstrated a better 10-year DSS compared to patients with low ATG4B expression (ATG4B H-score ≤ 150; denoted A-) (HR 0.78 (0.63–0.97), $p = 0.0250$). When all markers were combined, the most significant difference in survival in the L+ subset of patients was reached between the G-/L+/A- and G+/L+/A- groups, with the latter group demonstrating the worst prognosis (HR for 10-year

Table 3 Univariable association of LC3B expression with other markers and predictors of prognosis (validation cohort)

Variable	Levels	≤ 150 504	> 150 957	Total 1989	<i>p</i> value OneWay_Test
Diffuse expression (H-score > 150)					
Age at diagnosis	Mean (SE)	60 (1)	58 (0)	59 (0)	0.006
	Median (IQR)	61 (49–69)	58 (47–68)	59 (48–69)	
	Missing	0	0	0	
Tumor size (cm)	Mean (SE)	2 (0)	3 (0)	2 (0)	0.053
	Median (IQR)	2 (2–3)	2 (2–3)	2 (2–3)	
	Missing	1	7	16	
					PearsonChi_square
Tumor grade	Grade 1–2	228 (47%)	372 (40%)	600 (43%)	0.020
	Grade 3	258 (53%)	551 (60%)	809 (57%)	
	Missing	18	34	85	
Nodal status	Negative	293 (58%)	517 (54%)	810 (56%)	0.172
	Positive	211 (42%)	436 (46%)	647 (44%)	
	Missing	0	4	5	
ER	< 1%	93 (19%)	338 (35%)	431 (30%)	0.000
	≥ 1%	409 (81%)	617 (65%)	1026 (70%)	
	Missing	2	2	14	
PR	< 1%	189 (40%)	500 (55%)	689 (50%)	0.000
	≥ 1%	288 (60%)	413 (45%)	701 (50%)	
	Missing	27	44	216	
HER2	{0, 1+, 2+w/FISH –ve}	460 (93%)	772 (82%)	1232 (86%)	0.000
	{2+w/FISH+ve, 3+}	34 (7%)	165 (18%)	199 (14%)	
	Missing	10	20	97	
CK5/6	Negative	423 (96%)	752 (88%)	1175 (91%)	0.000
	Positive	16 (4%)	102 (12%)	118 (9%)	
	Missing	65	103	306	
EGFR	Negative	428 (94%)	697 (82%)	1125 (86%)	0.000
	Positive	28 (6%)	155 (18%)	183 (14%)	
	Missing	48	105	274	
Ki67	< 14%	326 (72%)	375 (43%)	701 (53%)	0.000
	≥ 14%	128 (28%)	497 (57%)	625 (47%)	
	Missing	50	85	266	
BCL2	Negative or ≤ 10%	81 (16%)	298 (32%)	379 (26%)	0.000
	Any staining and > 10%	415 (84%)	637 (68%)	1052 (74%)	
	Missing	8	22	164	
CA-IX	Negative	422 (90%)	725 (80%)	1147 (83%)	1e–05
	Any positive	49 (10%)	179 (20%)	228 (17%)	
	Missing	33	53	181	
HER3 (any staining)	No staining	394 (95%)	657 (86%)	1051 (89%)	0.000
	Any staining	22 (5%)	109 (14%)	131 (11%)	
	Missing	88	191	431	
IGF1R (Allred ≥ 7)	< 7	273 (59%)	482 (55%)	755 (56%)	0.171
	≥ 7	193 (41%)	402 (45%)	595 (44%)	
	Missing	38	73	337	
PD-L1 (≥ 1%)	< 1	436 (97%)	774 (89%)	1210 (92%)	0.000
	≥ 1	12 (3%)	95 (11%)	107 (8%)	
	Missing	56	88	534	

Table 3 (continued)

					PearsonChi_ square
Basal	Non-basal	435 (96%)	773 (86%)	1208 (90%)	0.000
	Basal	18 (4%)	123 (14%)	141 (10%)	
	Missing	51	61	273	
Triple-negative	Not TNP	446 (90%)	748 (79%)	1194 (83%)	0.000
	TNP	48 (10%)	197 (21%)	245 (17%)	
	Missing	10	12	84	
IHC subtype	lumA	283 (62%)	294 (33%)	577 (43%)	0.000
	lumB/ki67 high	88 (19%)	247 (28%)	335 (25%)	
	lumB/HER2+	17 (4%)	65 (7%)	82 (6%)	
	HER2+/ER–/PR–	17 (4%)	93 (10%)	110 (8%)	
	Basal	18 (4%)	123 (14%)	141 (10%)	
	add'l TNP	30 (7%)	74 (8%)	104 (8%)	
ATG4B (H-score > 150)	Missing	51	61	273	0.024
	≤ 150	356 (81%)	667 (75%)	1023 (77%)	
	> 150	85 (19%)	222 (25%)	307 (23%)	
GABARAP (H-score > 175)	Missing	63	68	572	0.000
	≤ 175	288 (60%)	193 (21%)	481 (34%)	
	> 175	193 (40%)	747 (79%)	940 (66%)	
LC3B (puncta low/neg)	Missing	23	17	423	0.000
	{D,E}	352 (70%)	202 (21%)	554 (38%)	
	{A,B,C}	152 (30%)	755 (79%)	907 (62%)	
Adjuvant systemic therapy	Missing	0	0	528	0.021
	No AST	215 (43%)	401 (42%)	616 (42%)	
	TAM only	177 (35%)	271 (28%)	448 (31%)	
	Chemo only	84 (17%)	201 (21%)	285 (20%)	
	TAM + chemo	25 (5%)	77 (8%)	102 (7%)	
	Ovarian ablation or horm other than TAM; no chemo	1 (0%)	4 (0%)	5 (0%)	
Ovarian ablation or horm other than TAM + chemo	2 (0%)	3 (0%)	5 (0%)		
Variable	Levels	{A,B,C}	{D,E}	Total	<i>p</i> value
	<i>N</i>	907	554	1989	OneWay_Test
LC3B (puncta low/neg)					
Age at diagnosis	Mean (SE)	58 (0)	59 (1)	59 (0)	0.079
	Median (IQR)	59 (47–69)	60 (48–69)	59 (48–69)	
	Missing	0	0	0	
Tumor size (cm)	Mean (SE)	3 (0)	2 (0)	2 (0)	0.467
	Median (IQR)	2 (2–3)	2 (2–3)	2 (2–3)	
	Missing	6	2	16	
					PearsonChi_ square
Tumor grade	Grade 1–2	346 (40%)	254 (47%)	600 (43%)	0.005
	Grade 3	527 (60%)	282 (53%)	809 (57%)	
	Missing	34	18	85	
Nodal status	Negative	486 (54%)	324 (58%)	810 (56%)	0.092
	Positive	417 (46%)	230 (42%)	647 (44%)	
	Missing	4	0	5	

Table 3 (continued)

					PearsonChi_ square
ER	< 1%	313 (35%)	118 (21%)	431 (30%)	0.000
	≥ 1%	592 (65%)	434 (79%)	1026 (70%)	
	Missing	2	2	14	
PR	< 1%	482 (56%)	207 (40%)	689 (50%)	0.000
	≥ 1%	386 (44%)	315 (60%)	701 (50%)	
	Missing	39	32	216	
HER2	{0, 1 +, 2 + w/FISH – ve}	737 (83%)	495 (92%)	1232 (86%)	0.000
	{2 + w/FISH + ve, 3 +}	154 (17%)	45 (8%)	199 (14%)	
	Missing	16	14	97	
CK5/6	Negative	729 (89%)	446 (93%)	1175 (91%)	0.026
	Positive	86 (11%)	32 (7%)	118 (9%)	
	Missing	92	76	306	
EGFR	Negative	664 (82%)	461 (93%)	1125 (86%)	0.000
	Positive	146 (18%)	37 (7%)	183 (14%)	
	Missing	97	56	274	
Ki67	< 14%	374 (45%)	327 (66%)	701 (53%)	0.000
	≥ 14%	455 (55%)	170 (34%)	625 (47%)	
	Missing	78	57	266	
BCL2	Negative or ≤ 10%	281 (31%)	98 (18%)	379 (26%)	0.000
	Any staining and > 10%	612 (69%)	440 (82%)	1052 (74%)	
	Missing	14	16	164	
CA-IX	Negative	685 (80%)	462 (89%)	1147 (83%)	1e–04
	Any positive	168 (20%)	60 (11%)	228 (17%)	
	Missing	54	32	181	
HER3 (any staining)	No staining	625 (86%)	426 (94%)	1051 (89%)	1e–05
	Any staining	105 (14%)	26 (6%)	131 (11%)	
	Missing	177	102	431	
IGF1R (Allred ≥ 7)	< 7	464 (55%)	291 (58%)	755 (56%)	0.194
	≥ 7	387 (45%)	208 (42%)	595 (44%)	
	Missing	56	55	337	
PD-L1 (≥ 1%)	< 1	739 (90%)	471 (95%)	1210 (92%)	0.004
	≥ 1	81 (10%)	26 (5%)	107 (8%)	
	Missing	87	57	534	
Basal	Non-basal	742 (88%)	466 (93%)	1208 (90%)	0.002
	Basal	106 (12%)	35 (7%)	141 (10%)	
	Missing	59	53	273	
Triple-negative	not TNP	723 (81%)	471 (87%)	1194 (83%)	0.004
	TNP	173 (19%)	72 (13%)	245 (17%)	
	Missing	11	11	84	
IHC subtype	lumA	292 (34%)	285 (57%)	577 (43%)	0.000
	lumB/ki67 high	236 (28%)	99 (20%)	335 (25%)	
	lumB/HER2+	57 (7%)	25 (5%)	82 (6%)	
	HER2+ /ER–/PR–	90 (11%)	20 (4%)	110 (8%)	
	basal	106 (12%)	35 (7%)	141 (10%)	
	add'l TNP	67 (8%)	37 (7%)	104 (8%)	
	Missing	59	53	273	

Table 3 (continued)

					PearsonChi_ square
ATG4B (H-score > 150)	≤ 150	639 (77%)	384 (77%)	1023 (77%)	0.870
	> 150	194 (23%)	113 (23%)	307 (23%)	
	Missing	74	57	572	
GABARAP (H-score > 175)	≤ 175	222 (25%)	259 (49%)	481 (34%)	0.000
	> 175	666 (75%)	274 (51%)	940 (66%)	
	Missing	19	21	423	
LC3B (H-score > 150)	≤ 150	152 (17%)	352 (64%)	504 (34%)	0.000
	> 150	755 (83%)	202 (36%)	957 (66%)	
	Missing	0	0	528	
Adjuvant systemic therapy	No AST	365 (40%)	251 (45%)	616 (42%)	0.175
	TAM only	274 (30%)	174 (31%)	448 (31%)	
	Chemo only	192 (21%)	93 (17%)	285 (20%)	
	TAM+chemo	69 (8%)	33 (6%)	102 (7%)	
	Ovarian ablation or horm other than TAM; no chemo	4 (0%)	1 (0%)	5 (0%)	
	Ovarian ablation or horm other than TAM+chemo	3 (0%)	2 (0%)	5 (0%)	

DSS was 1.51 (1.13–2.01), $p = 0.0038$; HR for 10-year PFS was 1.50 (1.06–2.19), $p = 0.0172$). Together, these analyses suggest that even though LC3B puncta has the strongest association with patient survival, further patient stratification may be possible by combining LC3B with GABARAP and ATG4B expression.

Discussion

We explored the differential expression and prognostic potential of three functionally related autophagy proteins, LC3B, GABARAP, and ATG4B, using tissue microarrays from a cohort of 3992 breast cancer patients. This is the first analysis of GABARAP and ATG4B in breast cancer patients and also the first study to quantitatively evaluate the punctate and diffuse staining patterns of LC3B with respect to prognostic value. Other groups previously evaluated biomarker potential of LC3B in breast cancer [30–33, 41, 42]. Only some of these studies [30–33] evaluated LC3B puncta in tumor cells, while others did not specify the pattern (diffuse or punctate) of LC3B staining that was assessed. Here, we analyzed both patterns of LC3B expression: diffuse (H-score), representing the cytoplasmic form of LC3B (LC3B-I), and punctate, representing the membrane-bound form of LC3B (LC3B-II). We established that

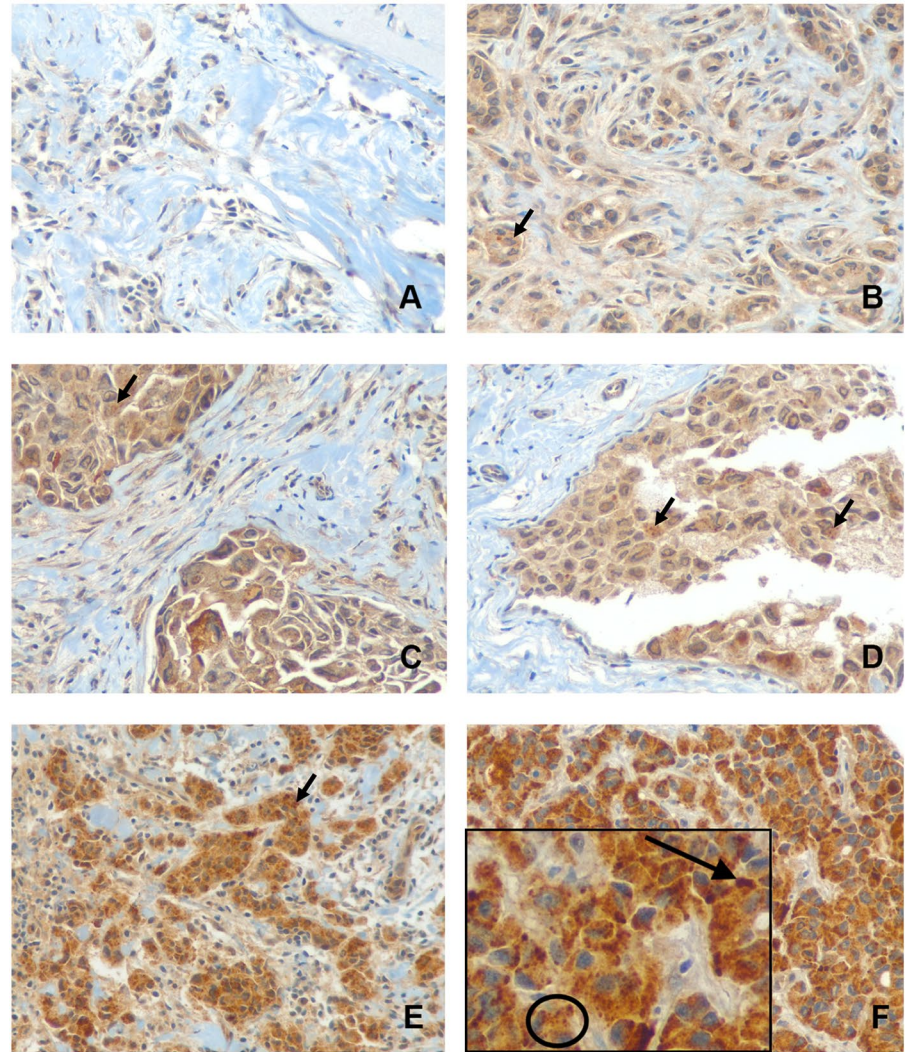
both LC3B staining patterns were associated with poor prognosis.

The highest LC3B and GABARAP expression levels were observed in basal-like breast cancers. It is possible that these patterns are a reflection of the previously reported high autophagy levels in basal-like breast cancers [38]. However, caution must be taken when interpreting these results with respect to autophagy status: high LC3B puncta expression has been linked to both autophagy induction (i.e., increased autophagosome formation) and autophagy inhibition (i.e., decreased lysosomal turnover). While additional assays evaluating autophagic flux [43–45] would be required to clarify the functional status of autophagy, this does not limit the potential biomarker utility of the observed staining patterns.

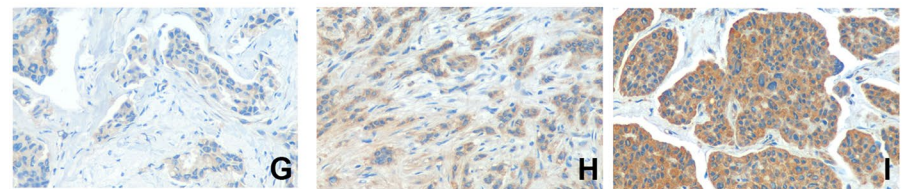
Overexpression of ATG4B was shown previously to cause extensive delipidation and interfere with efficient lysosomal fusion [14, 46], thereby suppressing autophagic flux. This observation suggests that relatively low levels of ATG4B may instead reflect active or functional autophagic flux. If so, then the low ATG4B expression coupled with the high LC3B/GABARAP expression in basal-like tumors may be indicative of increased autophagy levels in these tumors. It should be noted, however, that ATG4B expression levels are not necessarily equivalent to ATG4B activity levels. Recent reports evaluating ATG4B function in autophagy showed that post-translational modifications of ATG4B, such as phosphorylation, play important roles in regulating ATG4B

Fig. 1 Immunohistochemical staining showing expression of LC3B, ATG4B, and GABARAP in breast cancer patient samples. Representative images for LC3B cytoplasmic (H-score) and puncta (categorical) expression: **a** 100E; **b** 200D; **c** 200C; **d** 200B; **e** 300B; **f** 300A with zoomed-in image showing cells with high concentrations of individual puncta (circle) and clusters (long arrow). The short arrows in **b–e** point to puncta in tumor cells. Representative images for ATG4B expression (H-score): **g** 100; **h** 200; **i** 300. Representative images for GABARAP expression (H-score): **j** 100; **k** 200; **l** 300

LC3B



ATG4B



GABARAP

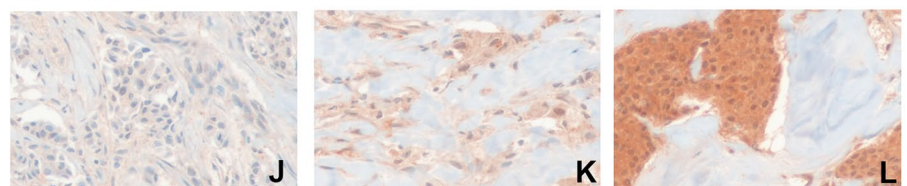


Fig. 2 Differential expression of ATG4B, GABARAP, and LC3B in breast cancer subtypes. H-score is indicated on the y axis and subtypes scored for each maker are shown across the x axis

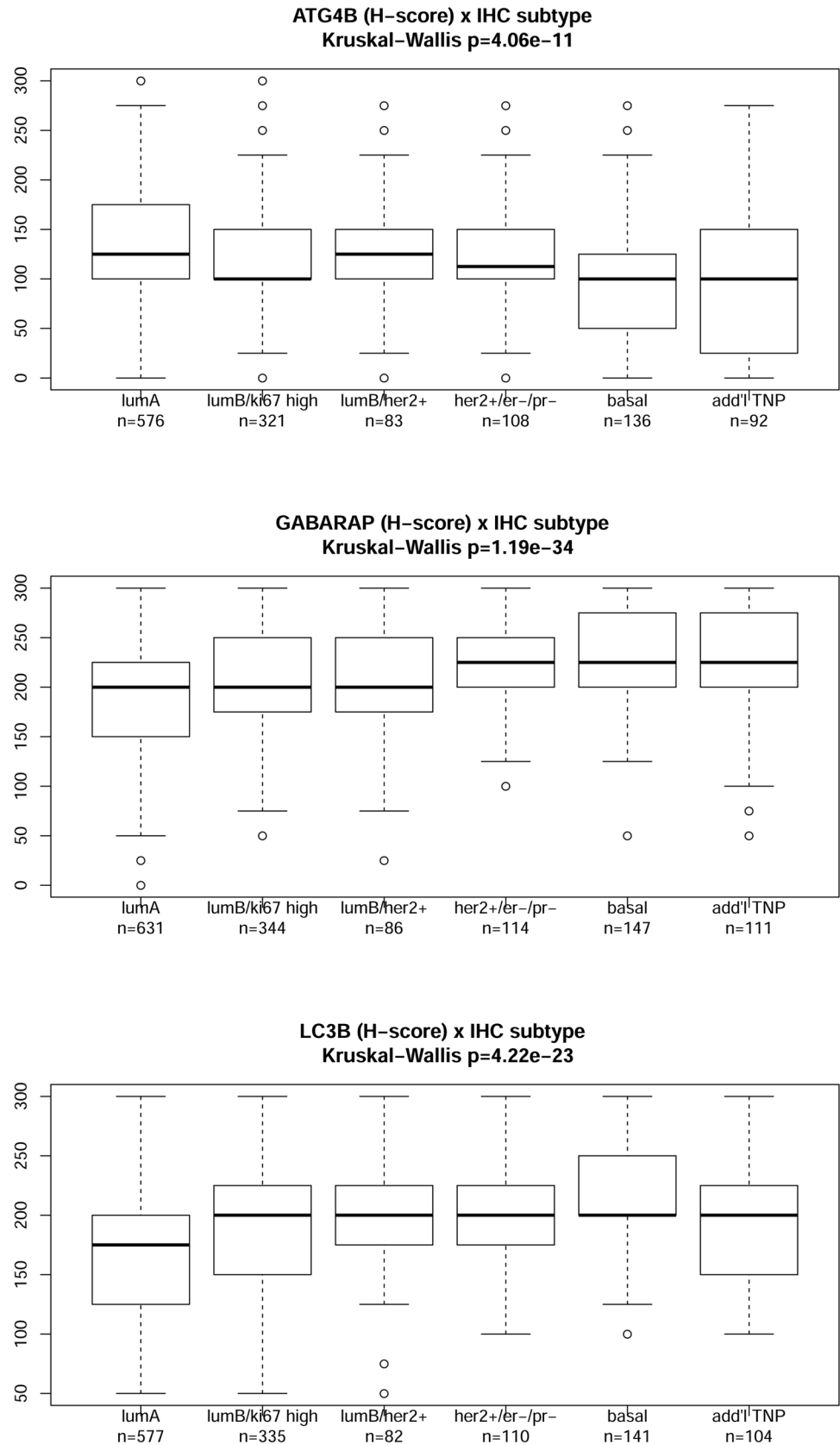
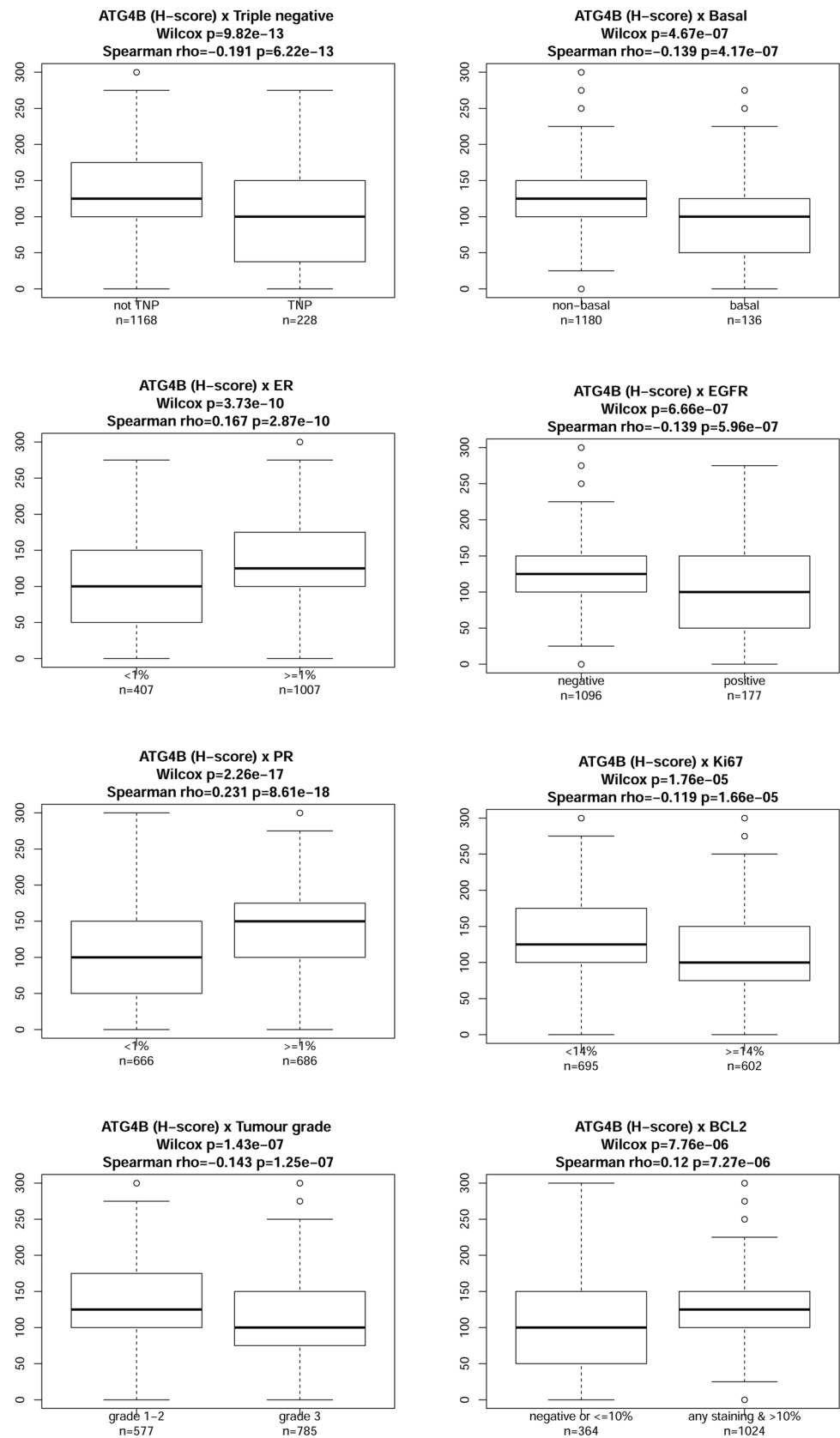


Fig. 3 Boxplots showing correlations of ATG4B with clinicopathological characteristics and biomarkers



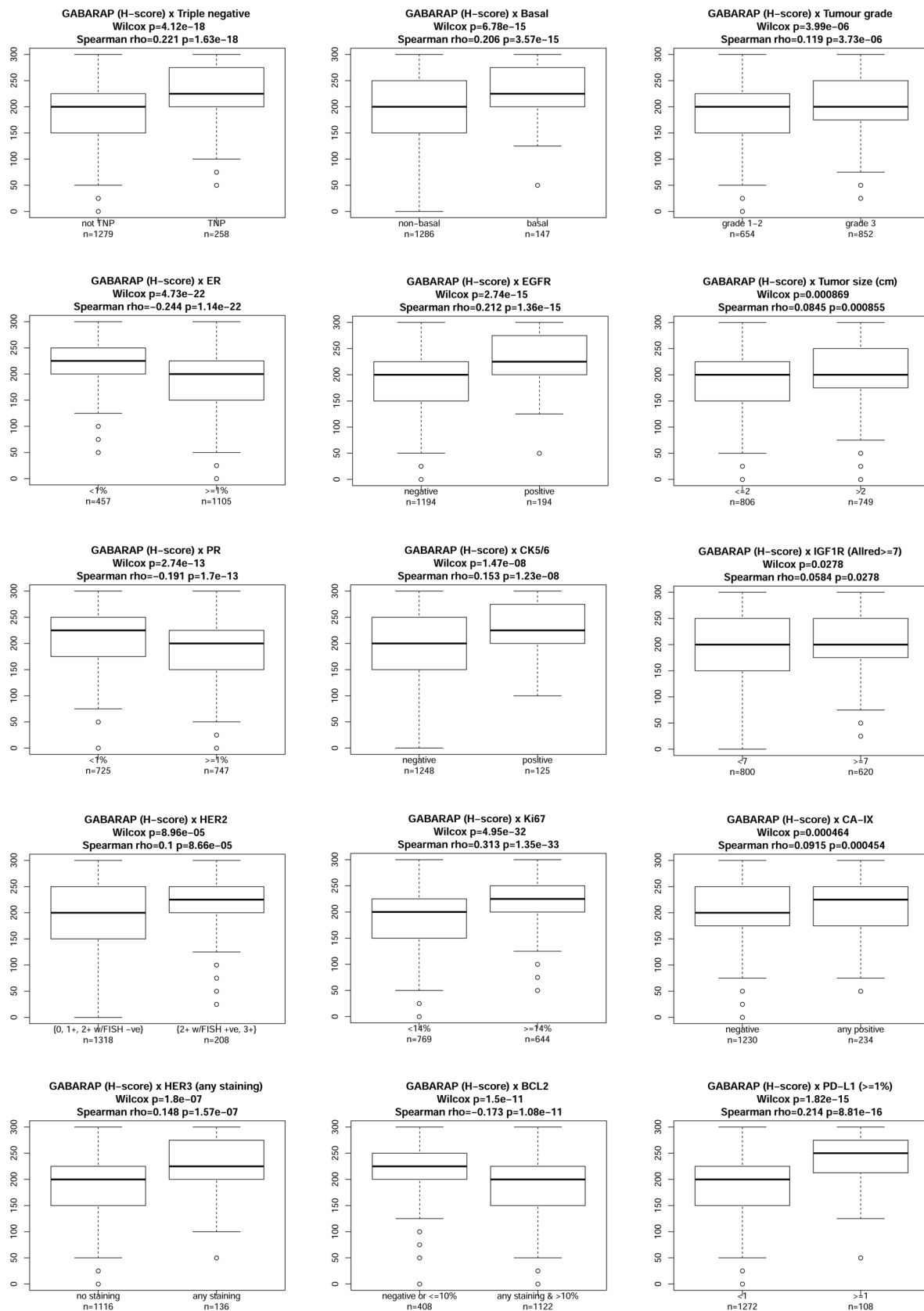


Fig. 4 Boxplots showing correlations of GABARAP with clinicopathological characteristics and biomarkers

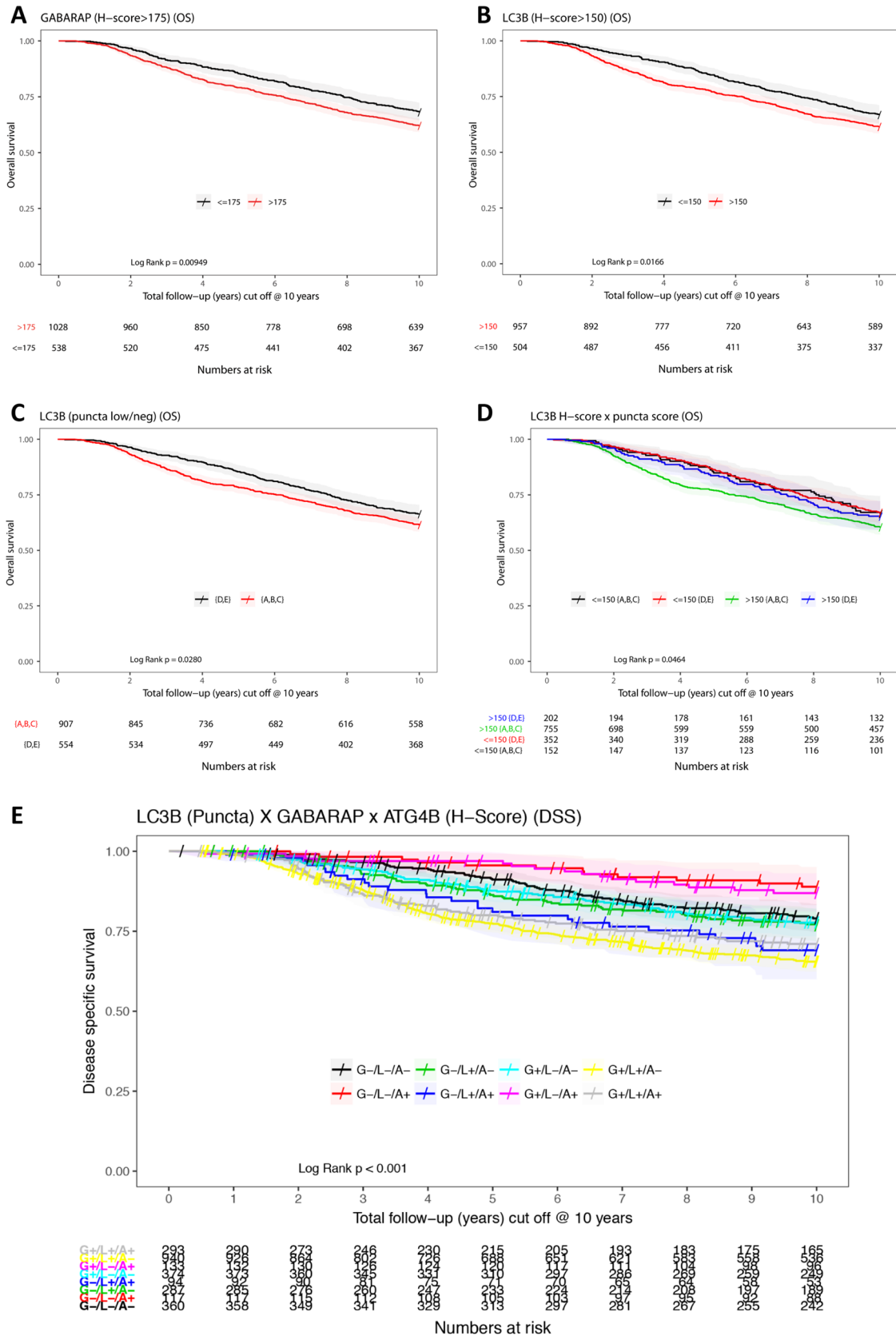


Fig. 5 Kaplan–Meier survival curves according to GABARAP expression (a), LC3B cytoplasmic expression (b), LC3B puncta expression (c), LC3B cytoplasmic and puncta expression combined (d) in the validation set. Exploratory analyses of the three markers (LC3B puncta, GABARAP, and ATG4B) combined (e) in the entire cohort. *L–low* (scored as D/E) LC3B expression, *L+high* (scored as A/B/C) LC3B expression, *G–low* (H-score < 175) GABARAP expression, *G+high* (H-score > 175) GABARAP expression, *A–low* (H-score < 150) ATG4B expression, *A+high* (H-score > 150) ATG4B expression

autophagic activity [47, 48]. Autophagy-independent roles of ATG4B have also been described [27, 28, 49]. One of the limitations of our study was the assessment of total, rather than phosphorylated, ATG4B levels in breast tumors, due to the unavoidable technical variability in surgical collection of human tumor tissues and the unreliability of phospho-antigens in formalin-fixed/paraffin-embedded specimens. In the future, it will be valuable to identify phosphorylation sites of ATG4B regulated in the context of breast cancer, and to assess their prognostic relevance, ideally in fresh-frozen tissue sections.

We found a number of significant associations among autophagy proteins and known breast cancer biomarkers. Both high LC3B expression and high GABARAP expression were associated with clinicopathological characteristics of aggressive disease phenotypes: high-grade tumors, ER/PR negativity, HER2 and HER3 positivity, high Ki67 (proliferation) index, and positive CK5/6 and EGFR expression. In contrast to LC3B and GABARAP, we found a negative correlation between the expression levels of ATG4B and the expression of poor prognostic markers such as Ki67, EGFR, and HER3. Each of these variables and markers has been previously described in relation to patient prognosis and cancer progression [50–58], but their association with LC3B, GABARAP, and ATG4B protein expression has not been reported previously.

We found statistically significant associations of LC3B and GABARAP expression with patient survival in univariable analyses. A number of previous reports [30–32, 41, 42] have also described an association of high LC3B expression with poor prognosis in breast cancer patients and the triple-negative (ER–, PR–, and HER2-negative) subtype, consistent with our findings on a much larger series. Other groups, however, indicated an opposite trend where LC3B negative expression correlated with adverse patient outcomes [32, 59]. Differences in patient cohort characteristics, including treatments received, intratumoral heterogeneity of LC3B expression, as well as staining and scoring techniques, may explain this discrepancy. Although LC3B puncta had the strongest association with patient prognosis, our exploratory multi-marker analysis indicated that further stratification by ATG4B and GABARAP expression may provide additional information regarding patient survival. Further studies to validate these marker combinations are required.

We overcame some of the known hurdles in the biomarker discovery process [60]—namely, sample size and follow-up time, but there are other limitations to our study. This large set of breast cancer TMAs was constructed from samples obtained from patients between 1986 and 1992. Even though many clinicopathological characteristics, such as tumor size, histological grade, ER/PR/HER2 status, Ki67 index, and intrinsic molecular subtype, remain relevant today, the treatment options available to patients have changed over time and shaped disease outcomes. This treatment aspect should be taken into consideration when interpreting the associations of GABARAP and LC3B with patient survival outcomes. To further validate these findings and determine independent prognostic marker potential, future studies should be performed on independent cohorts of patients, including those who received more modern treatments.

In summary, this is the largest cohort of breast cancer patients analyzed for LC3B biomarker value, and the first study to quantitatively evaluate its punctate versus diffuse staining patterns with respect to prognostic value. This is also the first analysis of GABARAP and ATG4B in breast cancer patients. Overall, we found that the differential expression of ATG4B did not associate with patient prognosis. High LC3B (punctate or diffuse) and high GABARAP expression associated with poor prognosis among all breast cancer subtypes, although multivariable analyses did not support either marker as an independent prognostic factor in this cohort. We also identified unique associations between known breast cancer biomarkers and these key autophagy proteins. Multi-marker analyses suggest that the combination of ATG4B and GABARAP with LC3B could be useful for further stratifying patient outcomes. This multi-marker approach and its biomarker potential warrant further investigation.

Methods

Study population

The study cohort included $n = 3992$ (interpretable cases $n = 2876$, $n = 2826$, and $n = 3122$ for LC3B, ATG4B, and GABARAP, respectively) patients initially diagnosed and seen at the British Columbia Cancer Agency between 1986 and 1992. This large, well-characterized cohort was described previously [61]; see Supplementary Methods. The study cohort was split into training and validation sets (see Supplementary Table S1). The training set was randomly selected to include 50% of the total study population and was used to identify optimal cutoff points as well as biomarker associations and prognostic trends, which were then tested on the remaining 50% (validation set) of the study population. All values described in the text are based on the

Table 4 Univariable analyses of relation of GABARAP and LC3B status to OS/DSS/RFS among validation cohort

	# of events/n	Hazard ratio (95% CI)	LRT <i>p</i> value
Cutoff at 18 years			
GABARAP (H-score > 175)			
OS	746/1566	1.12 (0.96–1.30)	0.140
DSS	441/1563	1.27 (1.04–1.56)	0.018
RFS	578/1566	1.12 (0.94–1.33)	0.199
LC3B (H-score > 150)			
OS	705/1461	1.16 (0.99–1.36)	0.058
DSS	419/1458	1.31 (1.07–1.61)	0.009
RFS	548/1461	1.12 (0.94–1.34)	0.204
LC3B (puncta low/neg)			
OS	705/1461	1.18 (1.01–1.37)	0.035
DSS	419/1458	1.28 (1.05–1.57)	0.014
RFS	548/1461	1.09 (0.92–1.30)	0.315
Cutoff at 10 years			
GABARAP (H-score > 175)			
OS	560/1566	1.27 (1.06–1.52)	0.009
DSS	373/1563	1.43 (1.15–1.80) ^F	0.001
RFS	522/1566	1.12 (0.93–1.34)	0.226
LC3B (H-score > 150)			
OS	535/1461	1.25 (1.04–1.50)	0.015
DSS	355/1458	1.42 (1.13–1.79)	0.002
RFS	497/1461	1.23 (1.02–1.49)	0.028
LC3B (puncta low/neg)			
OS	535/1461	1.22 (1.02–1.46)	0.027
DSS	355/1458	1.43 (1.14–1.79)	0.001
RFS	497/1461	1.14 (0.95–1.37)	0.149
Cutoff at 5 years			
GABARAP (H-score > 175)			
OS	294/1566	1.48 (1.15–1.92) ^F	0.002
DSS	218/1563	1.69 (1.25–2.32) ^F	< 0.001
RFS	382/1566	1.13 (0.91–1.40)	0.255
LC3B (H-score > 150)			
OS	278/1461	1.62 (1.25–2.14) ^F	< 0.001
DSS	205/1458	1.87 (1.36–2.61) ^F	< 0.001
RFS	363/1461	1.40 (1.11–1.76)	0.003
LC3B (puncta low/neg)			
OS	278/1461	1.56 (1.21–2.03) ^F	< 0.001
DSS	205/1458	1.99 (1.46–2.75) ^F	< 0.001
RFS	363/1461	1.41 (1.13–1.76)	0.002

validation cohort and include only those results that were significant in both training and validation sets.

Immunohistochemistry

Slices from the tissue microarray [61] (Supplementary Methods) were stained previously with a number of markers

including ER, PR, HER2, Ki67, CK5/6 and EGFR, as well as HER3, BCL2, IGF1R, CA-IX, and PD-L1 using procedures as described [50–58, 62, 63]. Intrinsic subtypes based on an immunohistochemical marker panel were assigned using the definitions previously published [50, 51]. ATG4B, GABARAP, and LC3B immunohistochemistry with anti-ATG4B (#A2981, Sigma), anti-GABARAP (#ab109364, Abcam), and anti-LC3B (#ab48394, Abcam) antibodies, respectively, was performed using the Ventana Discovery Ultra automated instrument (Ventana Medical Systems Inc, Tucson, USA) according to manufacturer's recommendations. Anti-ATG4B and anti-LC3B antibodies have been previously described [27, 30]; anti-GABARAP antibody was validated using GABARAP knock-out cell lines (See Supplementary Fig. S1 and Supplementary Methods).

Scoring and analysis of LC3B

Each sample was assessed by two independent observers for the intensity of cytoplasmic expression of LC3B in tumor cells under X20 objective magnification, as well as for the presence (i.e., positivity) of LC3B puncta under X40 objective magnification. LC3B cytoplasmic expression was scored using a H-score, consisting of multiplying cytoplasmic staining intensity of tumor cells (from 0 to 3) to the percentage of tumor cells staining (from 0 to 100%) which resulted in a score range of 0 to 300. The score was then categorized into 7 groups (0, 50, 100, 150, 200, 250, 300) by rounding to the closest multiple of 50. LC3B puncta expression was scored using a 5-point categorical scoring system: A. super high (clusters in > 50% of cells), B. high with some (< 50%) clusters, C. high puncta (in > 50% of cells), no clusters, D. low puncta (puncta in < 50% of cells), no clusters, E. negative (Fig. 1). For this purpose, a cluster refers to a dense accumulation of LC3B puncta (e.g., Fig. 1f) as opposed to more distinct individual puncta (e.g., Fig. 1c). All clinical and pathological data for each tumor sample were blinded to the scorers during scoring by two pathologists. The weighted Kappa values (0.71 for the H-score, and 0.66 for puncta scoring) indicated that substantial agreement between the two scores was achieved [64].

Scoring and analysis of ATG4B and GABARAP

Each sample was assessed for the presence (i.e., positivity) and intensity of cytoplasmic expression of ATG4B and GABARAP in tumor cells under X20 objective magnification. ATG4B and GABARAP cytoplasmic expression were scored using the same H-score, consisting of multiplying cytoplasmic staining intensity of tumor cells (from 0 to 3) to the percentage of tumor cells staining (from 0 to 100%) which resulted in a score range of 0 to 300. The score was then categorized into 7 groups (0, 50, 100, 150, 200, 250, 300) by rounding

Table 5 Multivariable survival analyses with ATG4B, GABARAP and LC3B puncta (validation set at 10 years)

Variable	# of events/ <i>n</i>	Comparison group	Hazard Ratio (95% CI)	LRT <i>p</i> value
OS (10 years)	415/1143			
ATG4B (H-score > 150) (reference group: ≤ 150)		> 150	1.13 (0.90–1.43)	0.296
GABARAP (H-score > 175) (reference group: ≤ 175)		> 175	1.09 (0.87–1.36)	0.471
LC3B (puncta low/neg) (reference group: {D,E})		{A,B,C}	1.01 (0.81–1.25)	0.946
Age at diagnosis (reference group: < 50)		≥ 50	1.70 (1.27–2.28)	< 0.001
Tumor grade (reference group: grade 1–2)		Grade 3	1.46 (1.16–1.82)	< 0.001
Tumor size (cm) (reference group: ≤ 2)		> 2	1.41 (1.15–1.73)	< 0.001
Lymphovascular invasion (reference group: negative)		Positive	1.34 (1.05–1.70)	0.016
Nodal status (reference group: negative)		Positive	1.95 (1.50–2.52)	< 0.001
IHC subtype (reference group: lumA)		lumB/ki67 high	1.51 (1.17–1.96)	0.022
		lumB/HER2+	1.53 (1.04–2.25)	
		HER2+ /ER– /PR–	1.42 (0.98–2.06)	
		Basal	1.60 (1.13–2.28)	
		add'l TNP	1.43 (0.93–2.19)	
Adjuvant systemic therapy (reference group: no AST)		TAM only	0.69 (0.51–0.92)	0.009
		Chemo only	0.60 (0.41–0.88)	
		TAM + chemo	0.46 (0.28–0.75)	
		Ovarian ablation or horm other than TAM; no chemo	2.84 (0.68–11.84)	
		Ovarian ablation or horm other than TAM + chemo	0.49 (0.07–3.66)	
DSS (10 years)	281/1140			
ATG4B (H-score > 150) (reference group: ≤ 150)		> 150	1.01 (0.75–1.35) ^F	0.952
GABARAP (H-score > 175) (reference group: ≤ 175)		> 175	1.17 (0.89–1.56) ^F	0.250
LC3B (puncta low/neg) (reference group: {D,E})		{A,B,C}	1.08 (0.83–1.41) ^F	0.556
Age at diagnosis (reference group: < 50)		≥ 50	1.04 (0.74–1.46) ^F	0.827
Tumor grade (reference group: grade 1–2)		grade 3	1.81 (1.36–2.43) ^F	< 0.001
Tumor size (cm) (reference group: ≤ 2)		> 2	1.60 (1.24–2.07) ^F	< 0.001
Lymphovascular invasion (reference group: negative)		Positive	1.47 (1.10–1.99) ^F	0.009
Nodal status (reference group: negative)		Positive	2.43 (1.77–3.36) ^F	< 0.001
IHC subtype (reference group: lumA)		lumB/ki67 high	1.49 (1.07–2.07) ^F	0.036
		lumB/HER2+	1.58 (0.99–2.45) ^F	
		HER2+ /ER– /PR–	1.85 (1.20–2.83) ^F	
		Basal	1.81 (1.19–2.74) ^F	
		add'l TNP	1.52 (0.90–2.47) ^F	
Adjuvant systemic therapy (reference group: no AST)		TAM only	0.74 (0.51–1.07) ^F	0.109
		Chemo only	0.57 (0.36–0.88) ^F	
		TAM + chemo	0.52 (0.29–0.89) ^F	
		Ovarian ablation or horm other than TAM; no chemo	1.10 (0.01-NA) ^F	
		Ovarian ablation or horm other than TAM + chemo	0.69 (0.08–2.79) ^F	

Table 5 (continued)

Variable	# of events/ <i>n</i>	Comparison group	Hazard Ratio (95% CI)	LRT <i>p</i> value
RFS (10 years)	398/1143			
ATG4B (H-score > 150) (reference group: ≤ 150)		> 150	0.99 (0.77–1.26) ^F	0.918
GABARAP (H-score > 175) (reference group: ≤ 175)		> 175	0.95 (0.76–1.19) ^F	0.679
LC3B (puncta low/neg) (reference group: {D,E})		{A,B,C}	0.97 (0.78–1.20) ^F	0.774
Age at diagnosis (reference group: < 50)		≥ 50	0.94 (0.71–1.23) ^F	0.641
Tumor grade (reference group: grade 1–2)		Grade 3	1.37 (1.09–1.72) ^F	0.006
Tumor size (cm) (reference group: ≤ 2)		> 2	1.56 (1.26–1.92) ^F	< 0.001
Lymphovascular invasion (reference group: negative)		Positive	1.30 (1.02–1.67) ^F	0.037
Nodal status (reference group: negative)		Positive	1.97 (1.51–2.59) ^F	< 0.001
IHC subtype (reference group: lumA)		lumB/ki67 high	1.32 (1.02–1.72) ^F	0.159
		lumB/HER2+	1.52 (1.02–2.21) ^F	
		HER2+ /ER– /PR–	1.49 (1.02–2.14) ^F	
		Basal	1.28 (0.89–1.83) ^F	
		add'l TNP	1.17 (0.74–1.78) ^F	
Adjuvant systemic therapy (reference group: no AST)		TAM only	0.66 (0.48–0.91) ^F	0.019
		Chemo only	0.62 (0.43–0.90) ^F	
		TAM + chemo	0.48 (0.29–0.76) ^F	
		Ovarian ablation or horm other than TAM; no chemo	0.69 (0.01–NA) ^F	
		Ovarian ablation or horm other than TAM + chemo	0.51 (0.06–1.99) ^F	

LRT likelihood ratio test, AST adjuvant systemic therapy

^FFirth's penalized maximum likelihood bias reduction method was used to estimate the hazard ratio

to the closest multiple of 50 (Fig. 1). All clinical and pathological data for each tumor sample were blinded to the two scorers during scoring. The weighted Kappa values (0.92 for ATG4B and 0.75 for GABARAP) indicated that almost perfect or substantial, respectively, agreement between the two scores was achieved [64]. GABARAP was also evaluated for a punctate pattern of expression, similar to LC3B. However, the GABARAP puncta were less distinct and independently deemed unreliable for scoring by two pathologists.

Statistical analysis

The associations of ATG4B and LC3B status with continuous variables (age, tumor size) were assessed using Welch's *t*-test (one-way analysis of variance with no assumption on homogeneity of variances) and the associations with other binarized or categorical variables (grade, nodal status, LVSI, and other IHC markers) were done using a Chi-square test. Correlation was assessed by Spearman correlation test. Survival analyses were performed using Kaplan–Meier plots and Cox proportional hazards regression models. Multivariable Cox proportional

hazard regression models were used to adjust the prognostic significance of ATG4B/GABARAP/LC3B with clinicopathological parameters. A split training/validation analysis approach was used as a mean to cross validate any findings and to mitigate against overfitting from data-driven cutpoint determination. The entire cohort was split into training ($n=2003$) and validation ($n=1989$) sets. Exploratory analyses were first performed on the training set to generate hypotheses that were subsequently tested on the validation set as internal cross validation. All effect estimates (such as hazard ratio) and *p* values reported in the text are based on the validation cohort and include only results that were found significant in both training and validation sets unless stated otherwise.

Cutpoint determination

A cutpoint was defined for each marker in this study (ATG4B, GABARAP and LC3B H-score) using the Akaike Information Criterion (AIC). To determine the optimal cutpoint, a univariable Cox model fit was generated on the

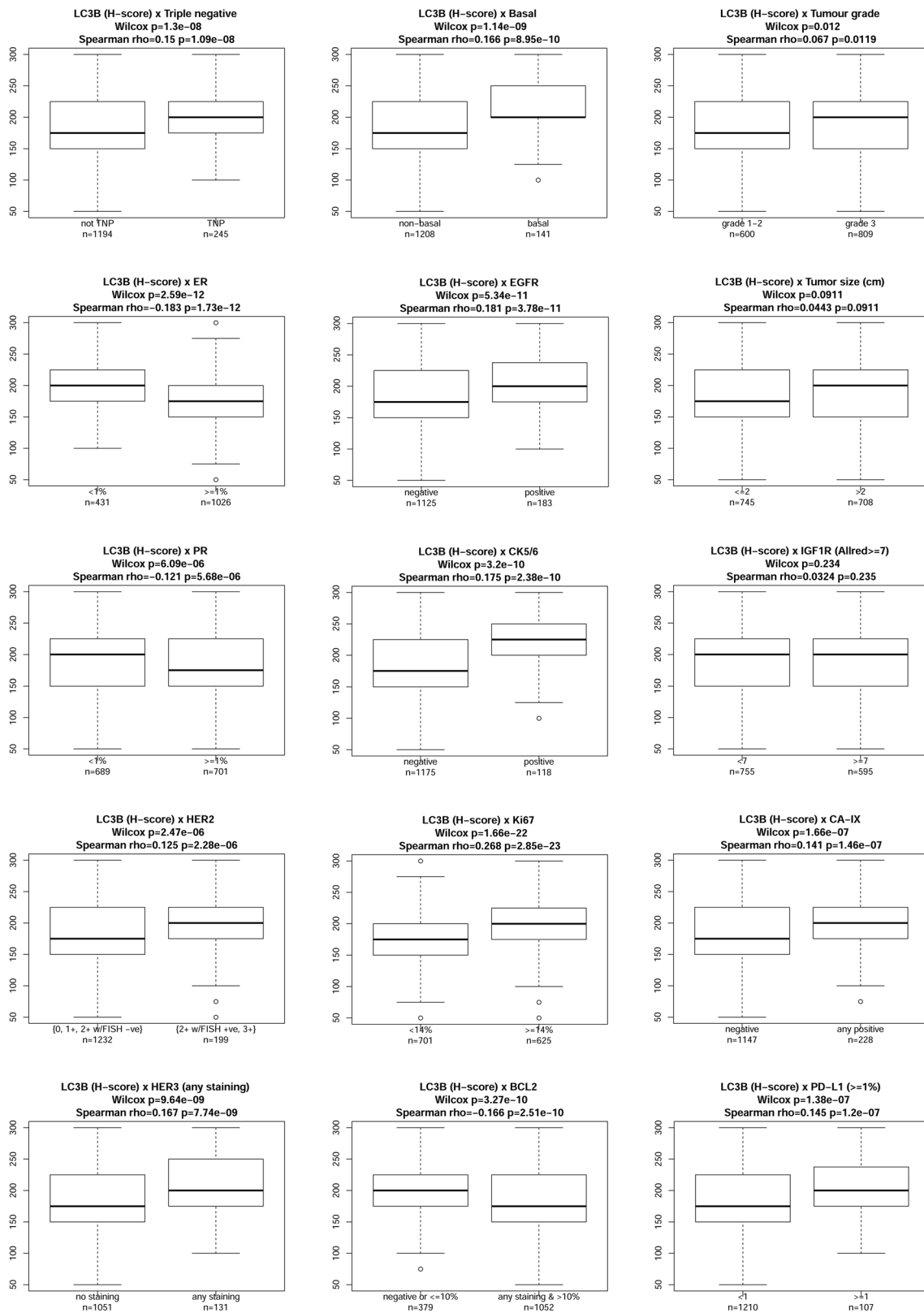


Fig. 6 Boxplots showing correlations of LC3B with clinicopathological characteristics and biomarkers

training set for all possible cutpoints and the corresponding AIC values calculated (see Supplementary Methods).

Acknowledgements We thank Christine Chow, Angela Cheng, and Rebecca Wu for technical support and members of the Gorski laboratory for helpful comments and discussions.

Author contributions SBo, KAG, and SMG conceived the study; SBo, BTC, and FD scored slides with assistance of JM and KG; SL, KA, and SBu performed statistical analyses; JX created KO lines and performed GABARAP antibody validation; SY and TN supervised scoring; KAG, TON, and SMG supervised and directed the study; SBo, BTC, and SL wrote the manuscript; all authors read, edited, and approved the final manuscript.

Funding This study was funded by CIHR in partnership with Avon Foundation for Women-Canada grant OBC127216 and CIHR PJT-159536 Grant to SMG. SBo was supported by a CIHR Frederick Banting and Charles Best Canada Graduate Scholarship Doctoral Award.

Data availability The datasets used and/or analyzed during the current study are available from the corresponding author on reasonable request.

Compliance with ethical standards

Conflict of interest TON reports a licensing agreement with Veracyte, Inc. regarding the PAM50 intrinsic subtype classifier, not used in this study. The other authors declare that they have no conflict of interest.

Ethical approval This study and our access to the de-identified human data were approved by the Research Ethics Board of the University of British Columbia, British Columbia Cancer Agency and Simon Fraser University. This article does not contain any studies with animals performed by any of the authors.

Informed consent No informed consent was needed as anonymized archival specimens were used in this study, according to the Canadian Tri-Council Policy Statement for ethical research involving human subjects.

References

- Galluzzi L, Pietrocola F, Bravo-San Pedro JM et al (2015) Autophagy in malignant transformation and cancer progression. *EMBO J* 34:856–880
- Amaravadi R, Kimmelman AC, White E (2016) Recent insights into the function of autophagy in cancer. *Genes Dev* 30:1913–1930
- Levy JMM, Towers CG, Thorburn A (2017) Targeting autophagy in cancer. *Nat Rev Cancer* 17:528–542
- Dolgin E (2019) Anticancer autophagy inhibitors attract “resurgent” interest. *Nat Rev Drug Discov* 18:408–410
- Ravikumar B, Sarkar S, Davies JE et al (2010) Regulation of mammalian autophagy in physiology and pathophysiology. *Physiol Rev* 90:1383–1435
- Yang Z, Klionsky DJ (2010) Mammalian autophagy: core molecular machinery and signaling regulation. *Curr Opin Cell Biol* 22:124–131
- Itakura E, Mizushima N (2010) Characterization of autophagosome formation site by a hierarchical analysis of mammalian Atg proteins. *Autophagy* 6:764–776
- Feng Y, He D, Yao Z et al (2014) The machinery of macroautophagy. *Cell Res* 24:24–41
- Mizushima N, Yoshimori T, Ohsumi Y (2011) The role of Atg proteins in autophagosome formation. *Annu Rev Cell Dev Biol* 27:107–132
- Nguyen TN, Padman BS, Usher J et al (2016) Atg8 family LC3/GABARAP proteins are crucial for autophagosome–lysosome fusion but not autophagosome formation during PINK1/Parkin mitophagy and starvation. *J Cell Biol* 251:857
- Weidberg H, Shvets E, Shpilka T et al (2010) LC3 and GATE-16/GABARAP subfamilies are both essential yet act differently in autophagosome biogenesis. *EMBO J* 29:1792–1802
- Shpilka T, Weidberg H, Pietrokovski S et al (2011) Atg8: an autophagy-related ubiquitin-like protein family. *Genome Biol* 12:226
- Schaaf MBE, Keulers TG, Vooijs MA et al (2016) LC3/GABARAP family proteins: autophagy-(un)related functions. *FASEB J* 30:3961–3978
- Tanida I, Sou Y, Ezaki J et al (2004) HsAtg4B/HsApg4B/autophagin-1 cleaves the carboxyl termini of three human Atg8 homologues and delipidates microtubule-associated protein light chain 3- and GABAA receptor-associated protein-phospholipid conjugates. *J Biol Chem* 279:36268–36276
- Satoo K, Noda NN, Kumeta H et al (2009) The structure of Atg4B–LC3 complex reveals the mechanism of LC3 processing and delipidation during autophagy. *EMBO J* 28:1341–1350
- Fujita N, Hayashi-Nishino M, Fukumoto H et al (2008) An Atg4B mutant hampers the lipidation of LC3 paralogues and causes defects in autophagosome closure. *Mol Biol Cell* 19:4651–4659
- Li M, Hou Y, Wang J et al (2011) Kinetics comparisons of mammalian Atg4 homologues indicate selective preferences toward diverse Atg8 substrates. *J Biol Chem* 286:7327–7338
- Kauffman KJ, Yu S, Jin J et al (2018) Delipidation of mammalian Atg8-family proteins by each of the four ATG4 proteases. *Autophagy* 14:992–1010
- Akin D, Wang SK, Habibzadegah-Tari P et al (2014) A novel ATG4B antagonist inhibits autophagy and has a negative impact on osteosarcoma tumors. *Autophagy* 10:2021–2035
- Kurdi A, Cleenewerck M, Vangestel C et al (2017) ATG4B inhibitors with a benzotropolone core structure block autophagy and augment efficiency of chemotherapy in mice. *Biochem Pharmacol* 138:150–162
- Rothe K, Lin H, Lin KBL et al (2014) The core autophagy protein ATG4B is a potential biomarker and therapeutic target in CML stem/progenitor cells. *Blood* 123:3622–3634
- Tran E, Chow A, Goda T et al (2013) Context-dependent role of ATG4B as target for autophagy inhibition in prostate cancer therapy. *Biochem Biophys Res Commun* 441:726–731
- Bosc D, Vezenkov L, Bortnik S et al (2018) A new quinoline-based chemical probe inhibits the autophagy-related cysteine protease ATG4B. *Sci Rep* 8:11653
- Fu Y, Hong L, Xu J et al (2018) Discovery of a small molecule targeting autophagy via ATG4B inhibition and cell death of colorectal cancer cells in vitro and in vivo. *Autophagy* 15:1–17
- Liu P-F, Tsai K-L, Hsu C-J et al (2018) Drug repurposing screening identifies tioconazole as an ATG4 inhibitor that suppresses autophagy and sensitizes cancer cells to chemotherapy. *Theranostics* 8:830–845
- Bortnik S, Choutka C, Horlings HM et al (2016) Identification of breast cancer cell subtypes sensitive to ATG4B inhibition. *Oncotarget* 7:66970–66988

27. Liu P-F, Leung C-M, Chang Y-H et al (2014) ATG4B promotes colorectal cancer growth independent of autophagic flux. *Autophagy* 10:1454–1465
28. Liu P-F, Hsu C-J, Tsai W-L et al (2017) Ablation of ATG4B suppressed autophagy and activated AMPK for cell cycle arrest in cancer cells. *Cell Physiol Biochem Int J Exp Cell Physiol Biochem Pharmacol* 44:728–740
29. Bortnik S, Gorski SM (2017) Clinical applications of autophagy proteins in cancer: from potential targets to biomarkers. *Int J Mol Sci* 18:1496
30. Lazova R, Camp RL, Klump V et al (2012) Punctate LC3B expression is a common feature of solid tumors and associated with proliferation, metastasis, and poor outcome. *Clin Cancer Res Off J Am Assoc Cancer Res* 18:370–379
31. Ladoire S, Chaba K, Martins I et al (2012) Immunohistochemical detection of cytoplasmic LC3 puncta in human cancer specimens. *Autophagy* 8:1175–1184
32. Lefort S, Joffre C, Kieffer Y et al (2014) Inhibition of autophagy as a new means of improving chemotherapy efficiency in high-LC3B triple-negative breast cancers. *Autophagy* 10:2122–2142
33. Ladoire S, Penault-Llorca F, Senovilla L et al (2015) Combined evaluation of LC3B puncta and HMGB1 expression predicts residual risk of relapse after adjuvant chemotherapy in breast cancer. *Autophagy* 11:1878–1890
34. Holt SV, Wyspianska B, Randall KJ et al (2011) The development of an immunohistochemical method to detect the autophagy-associated protein LC3-II in human tumor xenografts. *Toxicol Pathol* 39:516–523
35. Martinet W, Schrijvers DM, Timmermans J-P et al (2013) Immunohistochemical analysis of macroautophagy. *Autophagy* 9:386–402
36. Bertucci F, Finetti P, Cervera N et al (2008) How basal are triple-negative breast cancers? *Int J Cancer* 123:236–240
37. Perou CM (2011) Molecular stratification of triple-negative breast cancers. *Oncologist* 16(Suppl 1):61–70
38. Maycotte P, Gearheart CM, Barnard R et al (2014) STAT3-mediated autophagy dependence identifies subtypes of breast cancer where autophagy inhibition can be efficacious. *Cancer Res* 74:2579–2590
39. Maycotte P, Thorburn A (2014) Targeting autophagy in breast cancer. *World J Clin Oncol* 5:224–240
40. Hayes DF, Ethier S, Lippman ME (2006) New guidelines for reporting of tumor marker studies in breast cancer research and treatment: REMARK. *Breast Cancer Res Treat* 100:237–238
41. Zhao H, Yang M, Zhao J et al (2013) High expression of LC3B is associated with progression and poor outcome in triple-negative breast cancer. *Med Oncol Northwood Lond Engl* 30:475
42. Chen S, Jiang Y-Z, Huang L et al (2013) The residual tumor autophagy marker LC3B serves as a prognostic marker in local advanced breast cancer after neoadjuvant chemotherapy. *Clin Cancer Res Off J Am Assoc Cancer Res* 19:6853–6862
43. Klionsky DJ, Abdelmohsen K, Abe A et al (2016) Guidelines for the use and interpretation of assays for monitoring autophagy (3rd edition). *Autophagy* 12:1–222
44. Chittaranjan S, Bortnik S, Gorski SM (2015) Monitoring autophagic flux by using lysosomal inhibitors and western blotting of endogenous MAP1LC3B. *Cold Spring Harb Protoc* 2015:743–750
45. He H, Yang Y, Xiang Z et al (2016) A sensitive IHC method for monitoring autophagy-specific markers in human tumor xenografts. *J Biomark*. <https://doi.org/10.1155/2016/1274603>
46. Yu Z-Q, Ni T, Hong B et al (2012) Dual roles of Atg8–PE deconjugation by Atg4 in autophagy. *Autophagy* 8:883–892
47. Yang Z, Wilkie-Grantham RP, Yanagi T et al (2015) ATG4B (autophagin-1) phosphorylation modulates autophagy. *J Biol Chem* 290:26549–26561
48. Huang T, Kim CK, Alvarez AA et al (2017) MST4 phosphorylation of ATG4B regulates autophagic activity, tumorigenicity, and radioresistance in glioblastoma. *Cancer Cell* 32(840–855):e8
49. Liu P-F, Chen H-C, Cheng J-S et al (2019) Association of ATG4B and phosphorylated ATG4B proteins with tumorigenesis and prognosis in oral squamous cell carcinoma. *Cancers* 11:1854
50. Cheang MCU, Voduc D, Bajdik C et al (2008) Basal-like breast cancer defined by five biomarkers has superior prognostic value than triple-negative phenotype. *Clin Cancer Res Off J Am Assoc Cancer Res* 14:1368–1376
51. Cheang MCU, Chia SK, Voduc D et al (2009) Ki67 index, HER2 status, and prognosis of patients with luminal B breast cancer. *J Natl Cancer Inst* 101:736–750
52. Liu S, Chia SK, Mehl E et al (2010) Progesterone receptor is a significant factor associated with clinical outcomes and effect of adjuvant tamoxifen therapy in breast cancer patients. *Breast Cancer Res Treat* 119:53–61
53. Cheang MCU, Treaba DO, Speers CH et al (2006) Immunohistochemical detection using the new rabbit monoclonal antibody SP1 of estrogen receptor in breast cancer is superior to mouse monoclonal antibody 1D5 in predicting survival. *J Clin Oncol Off J Am Soc Clin Oncol* 24:5637–5644
54. Jensen KC, Turbin DA, Leung S et al (2008) New cutpoints to identify increased HER2 copy number: analysis of a large, population-based cohort with long-term follow-up. *Breast Cancer Res Treat* 112:453–459
55. Dawson S-J, Makretsov N, Blows FM et al (2010) BCL2 in breast cancer: a favourable prognostic marker across molecular subtypes and independent of adjuvant therapy received. *Br J Cancer* 103:668–675
56. Lou Y, McDonald PC, Oloumi A et al (2011) Targeting tumor hypoxia: suppression of breast tumor growth and metastasis by novel carbonic anhydrase IX inhibitors. *Cancer Res* 71:3364–3376
57. Chiu CG, Masoudi H, Leung S et al (2010) HER-3 overexpression is prognostic of reduced breast cancer survival: a study of 4046 patients. *Ann Surg* 251:1107–1116
58. Yerushalmi R, Gelmon KA, Leung S et al (2012) Insulin-like growth factor receptor (IGF-1R) in breast cancer subtypes. *Breast Cancer Res Treat* 132:131–142
59. Chang S-J, Ou-Yang F, Tu H-P et al (2016) Decreased expression of autophagy protein LC3 and stemness (CD44+/CD24-/low) indicate poor prognosis in triple-negative breast cancer. *Hum Pathol* 48:48–55
60. Goossens N, Nakagawa S, Sun X et al (2015) Cancer biomarker discovery and validation. *Transl Cancer Res* 4:256–269
61. Voduc D, Cheang M, Nielsen T (2008) GATA-3 expression in breast cancer has a strong association with estrogen receptor but lacks independent prognostic value. *Cancer Epidemiol Biomark Prev Publ Am Assoc Cancer Res* 17:365–373
62. Burugu S, Gao D, Leung S et al (2017) LAG-3+ tumor infiltrating lymphocytes in breast cancer: clinical correlates and association with PD-1/PD-L1+ tumors. *Ann Oncol Off J Eur Soc Med Oncol* 28:2977–2984
63. Chia S, Norris B, Speers C et al (2008) Human epidermal growth factor receptor 2 overexpression as a prognostic factor in a large tissue microarray series of node-negative breast cancers. *J Clin Oncol Off J Am Soc Clin Oncol* 26:5697–5704
64. McHugh ML (2012) Interrater reliability: the kappa statistic. *Biochem Med* 22:276–282

Publisher's Note Springer Nature remains neutral with regard to jurisdictional claims in published maps and institutional affiliations.